

3D X-ray Imaging in Life Science Research

An Introduction to Capturing the 3D Structure of Biological Specimens Using X-rays



5 mm



Seeing beyond

Date: March 2023

Since the discovery of X-rays in 1895 by Wilhelm Röntgen, X-ray imaging has not only established itself as a vital tool in medicine but as a valuable approach in many fields of biological research. X-ray imaging benefits a wide range of life science applications with the ability to visualize internal 3D structures without physically cutting the sample. Combined with the increase in available staining and mounting protocols, the number of peer reviewed life science publications invoking X-ray imaging has rapidly increased over the last decade and this trend is continuing.

How does X-ray imaging work?

The generation of 3D X-ray data can be done both at the synchrotron and using lab-based tools. In either case, the associated nomenclatures can be confusing since multiple names are interchangeably used to describe 3D X-ray imaging (e.g., CT, microCT, X-ray Microscopy, XRM, Synchrotron CT (SCT), X-ray CT). Despite the range of names, the underlying technique that is common to them all is X-ray computed tomography.

X-ray computed tomography describes the acquisition of 2D X-ray transmission images captured at multiple viewing angles (Figure 1) and reconstructed to create a 3D representation of the specimen (Figure 2). The resulting 3D dataset shows the spatial distribution of apparent material density. The key benefit is that this is done without physically sectioning the specimen.

Different parts of the X-ray spectrum are useful for different biological applications. 'Hard' X-rays have high energy ranging from 5 to 124 keV and are the most widely used X-rays for structural analysis, whereas 'soft' X-rays have energies below 5 keV and enable exciting insights into 3D cellular structure in cryogenically preserved specimens.

Imaging with Hard X-rays in Life Science Research

One of the earliest uses of X-ray tomography in life science research was the visualization and characterization of mineralized tissue. First introduced in the late 1980s¹, X-ray tomography has now become the standard way of evaluating bone morphometry and the community has established a key set of guidelines to ensure that acquisition, reconstruction, processing and analysis generate accurate



Figure 2 A 3D computed tomography dataset is reconstructed from the series of 2D projection images. Each of the 1601 2D projection images captured at different rotation angles of this mouse bone are used in the reconstruction of the 3D dataset to generate a 3D representation of the bone. Internal structure is revealed in the reconstructed data without needing to physically cut the specimen.

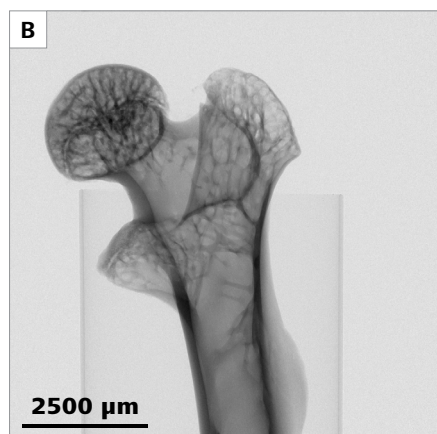
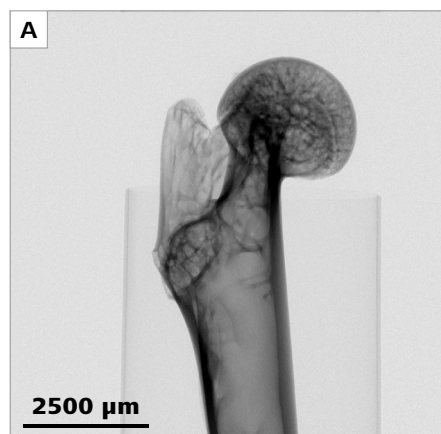


Figure 1 A 3D X-ray computed tomography dataset is generated from a series of 2D projection images of the specimen at different rotation angles. This mouse bone has been imaged at 1601 different rotation angles to generate a collection of 2D projection images. The single images (a and b) show two different 2D projections and the animation (c) shows all 1601 projection images combined.

and reproducible results². The composition of mineralized tissue means that structural imaging can often take place without the requirement of any staining or contrast enhancing approaches and this makes the sample preparation relatively straightforward. Parameters such as bone volume fraction (BV/TV), or cortical to trabecular bone ratio can be easily calculated from the X-ray tomography datasets (Figure 3) and multiscale experiments are now also unlocking new insights into bone structure and content³.

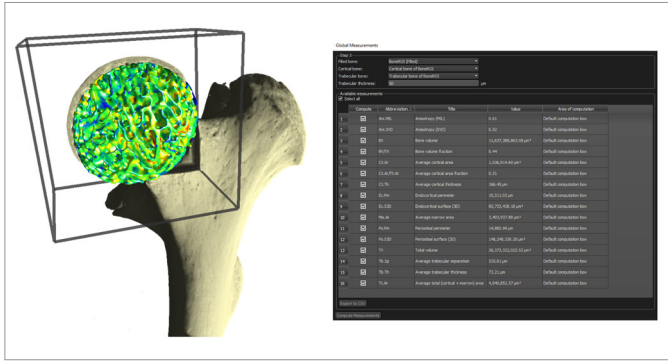


Figure 3 Non-destructive imaging using X-rays provides unique opportunities to capture the microstructure of bone and enables quantification of parameters such as trabecular and cortical bone fractions as well as a wide range of other parameters. The specimen is a dried mouse bone from the collection of Daniel Wescott, University of Texas at San Marcos. Image captured using ZEISS Xradia Versa and imagery and analysis performed using Dragonfly Pro Bone Analysis module with a subset of the calculated parameters shown in the table.

In addition to mineralized tissue, the value of using X-ray tomography to explore soft tissue specimens such as organs, organoids, tissue samples and skin is gaining traction.

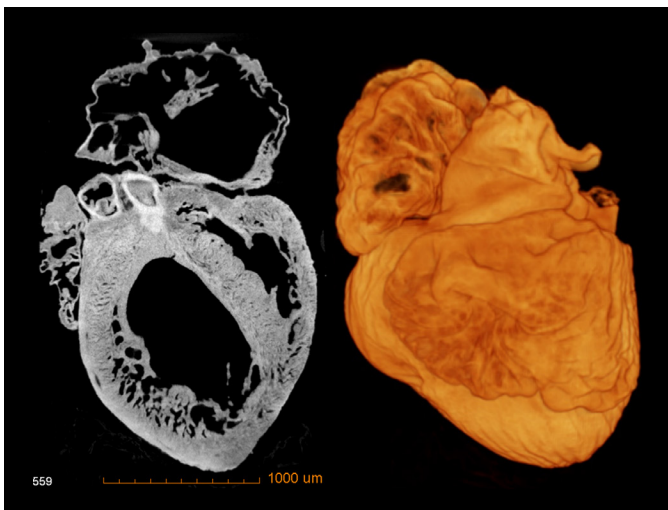


Figure 4 High resolution and contrast X-ray imaging in soft tissues like as the heart provide valuable insights into tissue structure such as differences between disease states or genetic models. The sample is a mouse embryonic heart imaged with the ZEISS Versa X-ray microscope. The image on the left shows a single section from the reconstructed dataset and the image on the right shows a rendering of the whole specimen in 3D. Sample courtesy of Dr. Chu Qing, Fuwai Hospital, Chinese Academy of Medical Sciences.

This is also true for whole organisms like zebrafish or mouse embryos, precious natural history specimens and a multitude of plant tissues (see examples in figures 4, 5, 6 and 10).

Find out more about non-destructive imaging using X-rays in life science specimens.

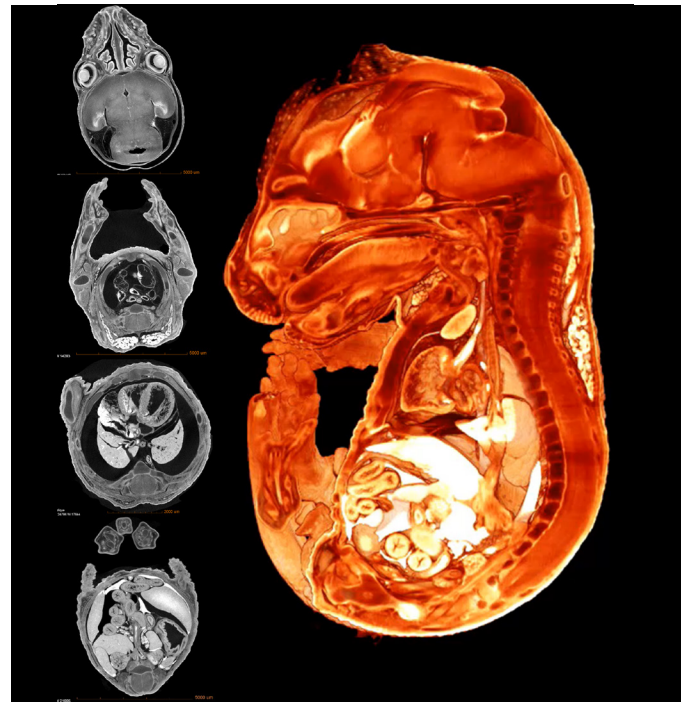


Figure 5 The internal structure of whole mouse models can be non-destructively assessed using X-ray imaging. High resolution and contrast enable detailed comparisons to be made between different groups; these can be useful for toxicology and developmental biology studies. The sample is a mouse embryo imaged with the ZEISS Xradia Versa X-ray microscope to reveal internal organs, bones and tissues. Sample courtesy of Dr Zheng Zhifa, Beijing Union Medical College Hospitals.

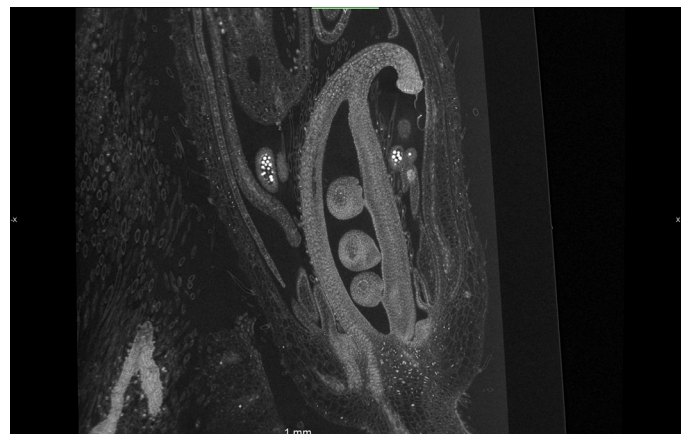


Figure 6 Using XRM for 3D visualization of plant biology both above and below the soil line provides a unique approach to specimen assessment that is not practical or possible using light or electron microscopy platforms. The sample is a soybean and the developing floral complex is imaged with the ZEISS Xradia Versa X-ray microscope. The tall ovary (pod) with the developing ovules (seeds), surround by the anthers that contain pollen grains (bright regions) can be seen. Scanning the specimens in this way is one of the most effective ways of appreciating the position of these important reproductive structures relate to each other in 3D space. Courtesy of Dr. Keith Duncan, Donald Danforth Plant Science Center, USA.

In vivo microCT imaging can provide insights into changing parameters in the live animal, often in combination with post sacrifice analysis of particular tissues using *ex vivo* tomography or complementary imaging approaches, such as light microscopy and/or electron microscopy.

Imaging with Soft X-rays in Life Science Research

'Soft' X-rays have energies below 5 keV. The enormous benefit for life science specimens when imaging with soft X-rays is the capacity to image within the 'water window'. This is a region of the electromagnetic spectrum between ~280–540 eV where water is relatively transparent to X-Rays but carbon is not. This unique combination affords the opportunity to image unstained organic molecules when preserved in their near to native state via cryo fixation (vitrification). In practice this means imaging 3D cellular ultrastructure in whole cells to a resolution of 25–40 nm⁴. The majority of soft X-ray facilities are provided by synchrotron beamlines (for example the facility at Diamond Light Source in the UK); however, lab-based soft X-ray systems are now also available and very often this approach for visualizing cellular ultrastructure can be combined with fluorescence or electron microscopy for correlative imaging and analysis^{4,5}. This is a rapidly moving field with great potential to provide a wealth of valuable insights in cell, viral and bacterial biology.

Find out more about soft X-ray imaging.

Instrument Configuration for 3D X-ray Tomography of Immobilized Samples

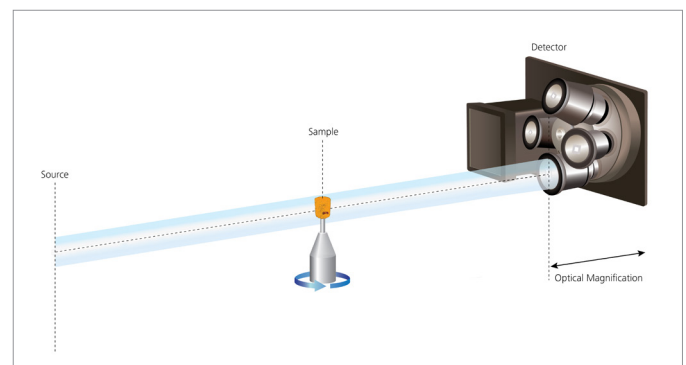
There are several instrument configuration variables that impact the final resolution and image quality of the reconstructed X-ray tomography data:

- Power, energy range and type of X-ray source
- Detection mechanism
- Magnification method

At the synchrotron, most X-ray tomography instruments for immobilized life science specimens use a collimated beam of high flux X-rays for imaging. Each beamline has its own unique end station configuration, but the majority use scintillators coupled to optics. The scintillators generate visible light from the X-rays that pass through the specimen, and this is then magnified using the objective lenses (analogous to a light microscope) before a high-resolution CCD camera captures the visible light to generate the projection image. The resolution of the image is primarily determined by the objective lens that is selected for each acquisition (Figure 7A).

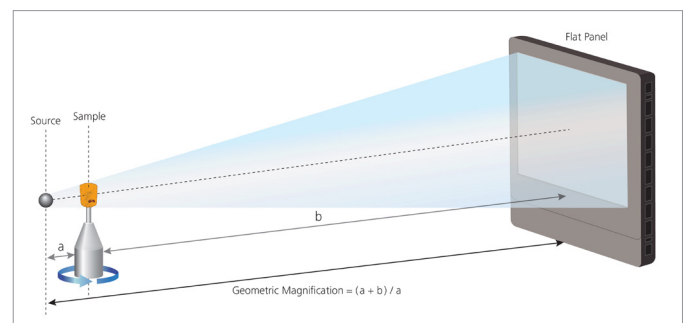
A) Common Synchrotron beamline configuration:

Collimated beam with optical magnification



B) Common microCT configuration:

Microfocus source and geometric magnification



C) X-ray microscopy configuration:

Microfocus source with both geometric and optical magnification

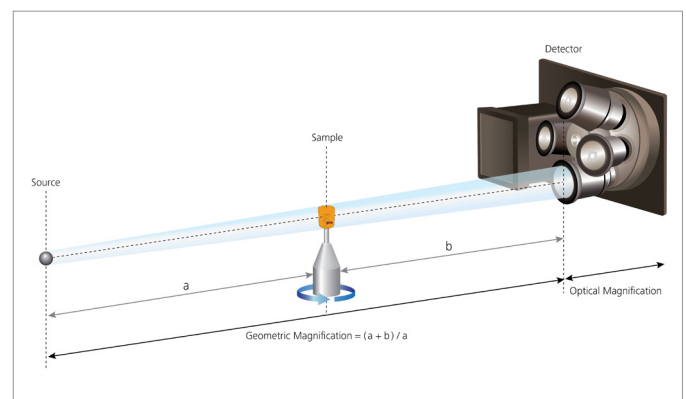


Figure 7 A comparison between different X-ray technologies. The majority of synchrotron end stations use optics to magnify the resulting image information (A). In lab-based microCT instruments, magnification is done using geometric magnification (physically moving the sample and source closer together), but this is ultimately limited by the sample dimensions (B). The lab-based X-ray microscope uses a combination of optical and geometric magnification to reach higher resolution in larger samples (C).

When moving to a lab-based CT or microCT system, the X-ray source is a micro-focussed spot which generates a cone or fan shaped X-ray beam. X-rays passing through the specimen are detected using flat panel X-ray detectors (or scintillator coated CCD cameras). To increase resolution, lab-based CT or microCT instruments rely on geometric magnification whereby resolution is increased by bringing the X-ray source and sample closer together and moving the detector further away. This magnification approach is effective, but resolution is limited since the source to sample distance is restricted by the bulk of the sample itself (Figure 7B).

An alternative lab-based instrument combines the optical technology employed at the synchrotron with the ease and portability of lab based microCT systems. These instruments are X-ray microscopes, and they provide high resolution and contrast without the need for applying for and waiting to use short periods of beamtime at the synchrotron. X-Ray microscopes use 2-stage magnification (using both geometric magnification and scintillator-coupled optical objective lenses) to enable multiscale imaging with the highest quality (Figure 7C). Additionally, X-ray microscopes can uniquely image interior volumes of specimens at much higher resolution than can be achieved using microCT. This allows researchers to gather the needed images without having to cut or section their specimen, preserving its integrity for further studies.

Generating Contrast in Life Science Specimens

Sample preparation, mounting and staining are key topics for any imaging approach using biological specimens, and X-ray imaging is no exception. For soft X-ray imaging, samples are prepared using vitrification approaches such as plunge freezing, and imaging takes place in the unstained specimen, usually on a grid. However, the relative low density of biological material means that when imaging with hard X-rays it can be challenging to generate sufficient contrast to visualize the structures of interest.

The way contrast is generated depends on the specimen. For example, the structure of mineralized tissue like as bone can often be captured without contrast agent since the difference in X-ray absorption between the bone tissue and surrounding material (e.g., soft tissue, liquid or air) is sufficient to generate the required contrast. However, for other specimens such as organs, soft tissue, plants, or embryos, invoking contrast agents to stain specimens can be of great benefit. Alternatively, contrast can be enhanced using critical point drying, which is particularly effective for insects, or corrosion cast imaging where the structures of interest are filled with material and the surrounding tissue is corroded. A review of the range of different contrast enhancing approaches is beyond the scope of this introduction but has been discussed elsewhere⁶ with more specific staining possibilities also under development.⁷

For specimens where the use of staining is unfeasible, but differences exist in X-ray refractive index (e.g., tissue membranes or a fossilized fly in amber), phase contrast can be employed as an alternative contrast method. In lab-based systems, propagation phase contrast can highlight the interface between components of the specimen with different X-ray refractive indices and these differences, when combined with absorption contrast, enable generation of a 3D image, even without staining (Figure 8). Having both absorption and propagation phase contrast acquisition available ensures the optimal choice of imaging approach for each specimen.

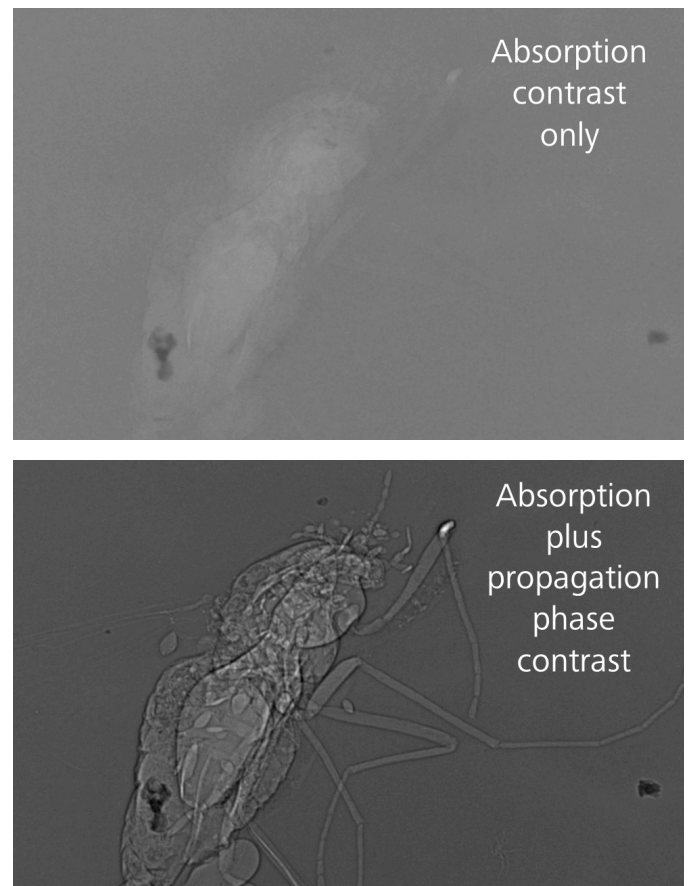


Figure 8 Absorption contrast alone may be insufficient to generate meaningful images if differences in absorption of materials within the specimen are very small. When using propagation phase contrast and absorption contrast together, differences in X-ray refractive index between sample components can be highlighted, which generates a clear representation of the specimen structure in 3D even without significant differences in density. Images captured using the ZEISS Versa X-ray microscope. The sample is a fossilized fly in amber.

Phase contrast imaging is possible due to the wave nature of X-rays which can be refracted by interfaces as they travel through the sample. As shown in figure 8, phase contrast imaging can be vital in uncovering specimen details. However, in revealing the X-ray refraction interfaces, phase contrast also generates dark and light bands, and this can make subsequent segmentation steps challenging. In cases where segmentation is required, the impact of phase contrast can also be minimized using post-acquisition processing approaches such as PhaseEvolve.

In addition to the multiple uses of phase imaging in lab-based instruments, exciting developments are also taking place at the synchrotron where phase contrast imaging is being used for capturing the structure of complete, unstained human organs⁸. This and similar examples are really showcasing the latest possibilities and are paving the way for generation of increasing numbers of novel insights from unstained specimens.

Minimizing X-ray Tomography Artifacts

X-ray tomography data can be prone to artifacts and care needs to be taken to minimize the impact of these on the resulting data. For lab-based instruments, the most common of these artifacts is beam hardening, which is caused by the differential absorption of high and low energy photons by the sample. Laboratory based X-ray tomography instruments use polychromatic X-ray sources which produce a range of X-ray energies. As the polychromatic X-rays pass through the sample, the relative absorption of high and low energy X-rays differs, with the high energy portion of the beam passing through the sample more easily and the lower-energy portion being preferentially stopped. The result is an increase in the average energy of the X-ray beam; this is called beam hardening. This artefact can show up as inhomogeneous reconstructed intensity in uniform materials (a characteristic bright ring is typical) and can contribute to bright streaks across the image, particularly when imaging samples that contain very different densities, such as a titanium implant in bone or tissue (for example figure 9).

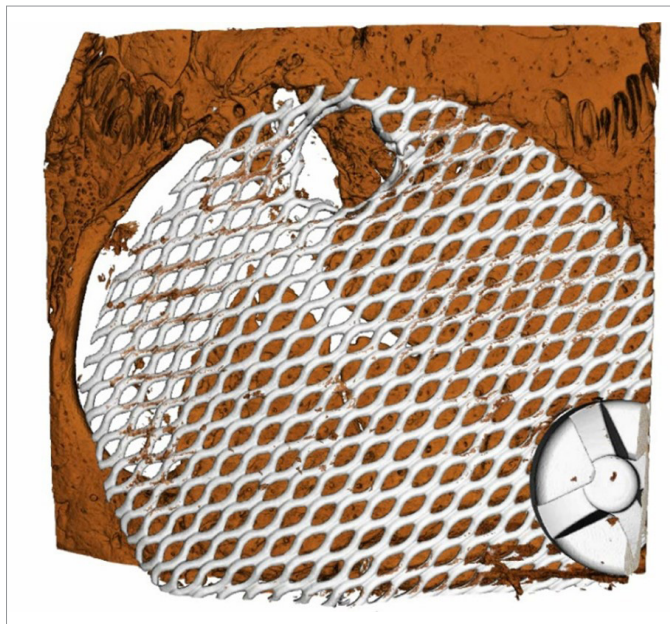


Figure 9 Quantifying the growth of new bone onto implants and scaffolds is important for understanding the biocompatibility of different materials and the efficacy of different implantation approaches. The sample is part of an injured rat skull that has been imaged using the ZEISS Xradia Versa X-ray microscope and the image is a 3D render of the dataset. The damaged area has been bridged with a titanium implant and the goal is to visualize the new bone growth into the implant area. The X-ray absorption of bone and titanium is very different. This can lead to challenges in terms of beam hardening when imaging with lab based instruments. Methods to minimize beam hardening can increase image quality for such specimens with significant differences in X-ray absorption.

Using a CT or microCT system, minimizing beam hardening artifacts can be done using physical filters to narrow the energy range of X-rays that is used for each sample. These filters, which are generally metals and ceramics, remove wavelength bands so these energies never reach the sample. Alternatively, post-acquisition processing algorithms can be invoked to decrease the artefact impact.

For the X-ray microscope, in addition to the physical filters, each of the optical objective lenses is coupled with a scintillator that is optimized for the energy range for which each objective is designed. This helps to minimize beam hardening since the energy range is optimally managed.

At the synchrotron, the energy range of the X-rays can be tightly controlled because the flux of X-rays is so high that selecting a small range (or even a single energy monochromatic beam) leaves more than enough flux for successful experiments. By removing the energy range, beam hardening artifacts are not a consideration at the synchrotron.

Ring artifacts also need to be controlled in 3D tomography imaging. Ring artifacts are usually caused by variations in the response from individual elements in a two-dimensional X-ray detector due to a defect or a miscalibration⁹.

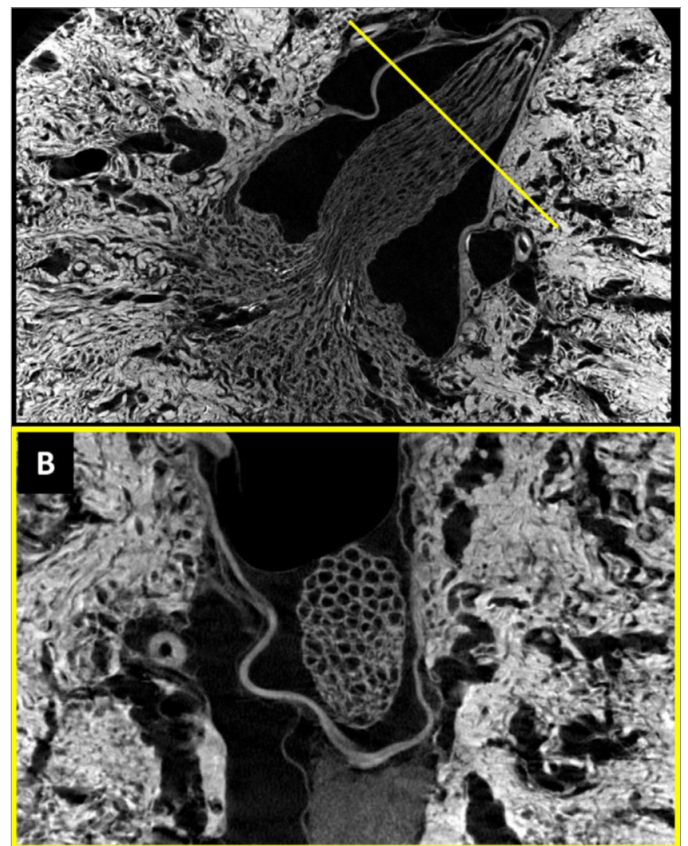


Figure 10 Visualizing the internal structure of organs can provide insights into different conditions or genetic disorders. The sample is a mouse kidney imaged with the ZEISS Xradia Versa X-ray microscope. The yellow line in the top image is the location for the cross section shown in B and focuses on the structure of the renal papilla.

Any fixed hardware challenge (such as a dead pixel on the detector for example) can lead to rings in the reconstructed datasets. Ring artifacts are very often corrected for using post acquisition filters or other post-processing methods¹⁰. Alternatively, smart acquisition routines whereby each projection image is captured several times, or subsequent projections are captured with the detector slightly shifted relative to the sample, minimize the probability of such artifacts.

Optimizing Reconstruction of X-ray Tomography Data

Reconstructing the hundreds to thousands of 2D X-ray projection images into a 3D volume demands powerful mathematical tools. The FDK algorithm, which was first proposed in 1984 for reconstructing images with a circular orbit of scan¹¹, is the most commonly used back-projection method for reconstruction. The FDK algorithm can generate good quality images in a fast and reliable reconstruction process and does not require as much computing power as other reconstruction methods such as iterative reconstruction. The FDK method, however, is sensitive to photon starvation and resulting images are prone to a variety of under-sampling artifacts. Consequently, a high number of projections, and/or long exposure times per projection are required for reducing image noise and artifacts which means long scans for high quality data acquisition.

Recent developments in reconstruction capability are being driven by advancements in computational power and machine learning to ultimately increase the speed of acquisition, signal to noise ratio and resolution in the resulting reconstruction. By generating a deep learning neural network model using patterns of expected reconstruction outcomes, it is now possible to reconstruct with the same image quality but with up to 10x fewer projections. Alternatively, the same approach can be used to increase the signal to noise ratio in the resulting 3D volume, which can be extremely powerful in specimens where the limits of the technology are being tested and high signal to noise data is required to answer the research question.

The very latest possibilities provided by deep learning are using high-resolution 3D microscopy datasets as training data for lower resolution, larger field of view datasets. This provides the opportunity to upscale the larger volume data using the neural network model to generate richer information at higher resolution.

[Find out more information here.](#)

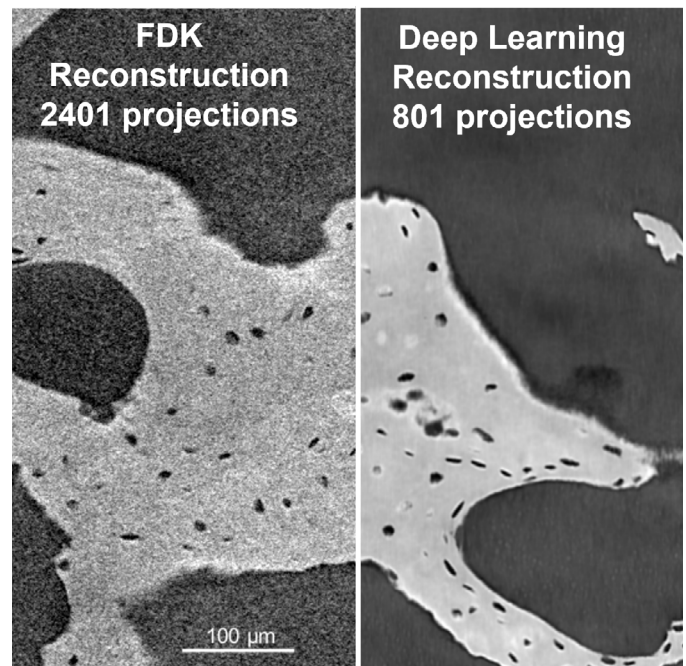


Figure 11 Reconstruction algorithms employing deep learning approaches can now provide significant improvements throughput by delivering an improvement in signal-to-noise ratio even with fewer 2D projection images. The image shows single 2D sections through reconstructed datasets acquired with 2401 projections on the left and 801 projection images on the right. The image on the left has been reconstructed using the traditional FDK algorithm, the image on the right has been reconstructed using deep learning (DeepRecon). The sample is dried mouse bone that has been imaged using the ZEISS Xradia Versa X-ray microscope.

Summary

A growing number of life science researchers now use X-ray tomography. As the technology advances, the increasing opportunities to gain insights with higher resolution and contrast are unlocking new applications. Careful consideration of sample preparation, staining and mounting ensures optimal results as well as selection of the right tool to provide the resolution, contrast, and sample management capabilities that each experiment demands. Technology developments in terms of X-ray source, detection capability and reconstruction approaches are pushing X-ray tomography to previously unreachable resolutions and it's an exciting time for those making the most of these advances both at the synchrotron and using lab-based instruments.

References

- [1] L. A. Feldkamp *et al.* (1989) **The direct examination of three-dimensional bone architecture in vitro by computed tomography.** *J Bone Miner Res.* 4:3–11, <https://doi.org/10.1002/jbmr.5650040103>
- [2] M. L. Bouxsein *et al.* (2010) **Guidelines for assessment of bone microstructure in rodents using micro-computed tomography.** *J Bone Miner Res.* 25(7):1468-86. <https://doi.org/10.1002/jbmr.141>
- [3] N. Kølln Wittig *et al.* (2022) **Opportunities for biomineralization research using multiscale computed X-ray tomography as exemplified by bone imaging.** *Journal of Structural Biology* 214 (1), <https://doi.org/10.1016/j.jsb.2021.107822>
- [4] M. Harkiolaki *et al.* (2018) **Cryo-soft X-ray tomography: using soft X-rays to explore the ultrastructure of whole cells.** *Emerg Top Life Science.* 2 (1): 81-92. <https://doi.org/10.1042/ETLS20170086>
- [5] I. Kounatidis *et al.* (2020) **3D Correlative Cryo-Structured Illumination Fluorescence and Soft X-ray Microscopy Elucidates Reovirus Intracellular Release Pathway.** *Cell* 182(2): 515-530.e17, <https://doi.org/10.1016/j.cell.2020.05.051>
- [6] B. D. Metscher. (2009) **MicroCT for comparative morphology: simple staining methods allow high-contrast 3D imaging of diverse nonmineralized animal tissues.** *BMC Physiol.* 9: 11. <https://doi.org/10.1186/1472-6793-9-11>
- [7] B. D. Metscher. (2021) **A simple nuclear contrast staining method for microCT-based 3D histology using lead (II) acetate.** *Journal of Anatomy.* 238:1036–1041, <https://doi.org/10.1186/1472-6793-9-11>
- [8] C. L. Walsh *et al.* (2021) **Imaging intact human organs with local resolution of cellular structures using hierarchical phase-contrast tomography.** *Nat. Methods* 18: 1532–1541, <https://doi.org/10.1038/s41592-021-01317-x>
- [9] J. Diwaker. (2014) **Adaptive center determination for effective suppression of ring artifacts in tomography images.** *Applied Physics Letters* 105 (14): 143107, <https://doi.org/10.1063/1.4897441>
- [10] J. Sijbers and A. Postnov. (2004) **Reduction of ring artifacts in high resolution micro-CT reconstructions.** *Physics in Medicine and Biology* 49(14): N247-53. <https://doi.org/10.1088/0031-9155/49/14/N06>
- [11] L. A. Feldkamp *et al.* (1984) **Practical cone-beam algorithm.** *J. Opt. Soc. Am.* A1: 612-619. <https://doi.org/10.1364/JOSAA.1.000612>

Cover image

Sample courtesy of Y. Yagi, Massachusetts General Hospital



Carl Zeiss Microscopy GmbH

07745 Jena, Germany

microscopy@zeiss.com

<https://zeiss.ly/wp-xrm-in-life-science-research-xrm-ls-overview-23>